Overview of Generic HVDC-MMC Control under Unbalanced Grid Conditions

Anton Stepanov, Hani Saad, Jean Mahseredjian, Aurélien Wataré

***Abstract*--This paper presents a summary of generic Modular Multilevel Converter (MMC) control techniques that are applicable under unbalanced grid conditions, which is useful for modeling of realistic MMC stations for grid and protection studies. Different decoupling techniques for positive/negative sequences, current control loops and current reference strategies are presented and their performances are compared. In addition, an efficient controller for zero-sequence currents to eliminate DC side ripple is developed and validated.**

***Keywords*: HVDC transmission system, Modular Multilevel Converter (MMC), Voltage Source Converter (VSC), unbalanced AC fault, EMT-type software, sequence decoupling, current control, Proportional-Resonant, DC voltage ripple suppression.**

I. Introduction

MODULAR Multilevel Converter (MMC) (see Fig. 1) is a Voltage Source Converter (VSC) topology that has several advantages in comparison with other power converters [1]. By increasing the number of sub-modules (SMs) per phase, the filter requirements can be eliminated, scalability to higher voltages is easily achieved and reliability is improved. Switching frequency and transient peak voltages on IGBTs are lower in MMCs, as well as switched voltage (single SM voltage compared to V_{dc}), which reduces converter losses [2].

During normal operation, SMs can be inserted (if the switch s1 is ON and s2 is OFF) or bypassed (if the switch s1 is OFF and s2 is ON), producing either v_C (capacitor voltage, Fig. 1) or 0 voltage drop across its terminals. In such a manner, the desired AC voltage waveform is constructed [1].

Grid codes stipulate operation during unbalanced faults. Two current control techniques are usually used in such conditions: PI control in positive and negative dq-frames [3]-[6]; and Proportional-Resonant control in αβ-frame [7]-[9].

Different upper level control objectives can be adopted, such as injection of balanced positive sequence AC side currents, suppression of active and/or reactive power oscillations and others [3]-[5], [10]-[12].

During grid unbalance, double line frequency oscillations appear on the DC side. They propagate to other converter stations, which impacts their normal operation. This has been treated in [13], [14], but further developments are required.

This article presents an overview of the most popular control strategies for MMCs. Also, an efficient new controller for zero sequence currents to eliminate DC side ripple is developed and validated.

A practical test case of an HVDC-MMC transmission system is used to validate presented control strategies. Their performances under unbalanced AC fault conditions are compared and analyzed.

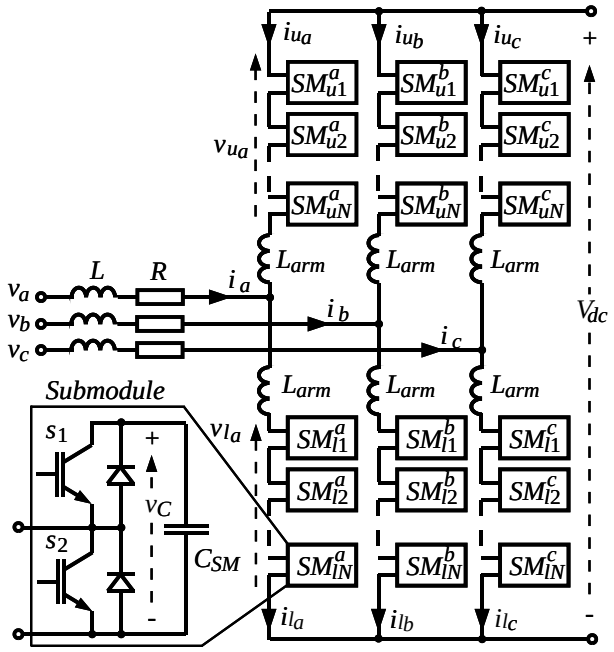

Fig. 1. Three-phase MMC topology with half-bridge submodules. L and R represent a transformer between the converter and the PCC

II. MMC Control

The control structure used in this paper is based on [15]. As this paper focuses on the development of control systems for unbalanced faults, only relevant control blocks are discussed in the next subsections: sequence extraction, PLL, current control, active/reactive power and DC voltage regulation, reference distribution and DC side double line frequency ripple suppression.

A. Sequence Extraction

In steady state, voltages and currents can be decomposed into positive, negative and zero sequences. In this article, AC side zero sequence is discarded due to natural filtering provided by D/Yn transformer between the MMC and the grid.

If positive "+" or negative "-" Park transformation is

A. Stepanov and J. Mahseredjian are with École Polytechnique de Montréal, Montréal, QC, Canada (e-mail of corresponding author: anton.stepanov@polymtl.ca, jeanm@polymtl.ca).

H. Saad and A. Wataré are with Réseau de Transport d'Electricité, Paris, France (e-mail: hani.saad@rte-france.com, aurelien.watare@rte-france.com).

Paper submitted to the International Conference on Power Systems Transients (IPST2017) in Seoul, Republic of Korea June 26-29, 2017

applied to a system that contains positive and negative sequences, a combination of a constant term and a term oscillating at double line frequency (2ω) is obtained:

$$\begin{bmatrix} x_d^+ \\ x_q^+ \end{bmatrix} = X^+ \begin{bmatrix} \cos\left(\phi^+ - \psi\right) \\ \sin\left(\phi^+ - \psi\right) \end{bmatrix} + X^- \begin{bmatrix} \cos\left(-2\omega t - \phi^- - \psi\right) \\ \sin\left(-2\omega t - \phi^- - \psi\right) \end{bmatrix} \quad (1)$$

$$\begin{bmatrix} x_d^- \\ x_q^- \end{bmatrix} = X^- \begin{bmatrix} \cos\left(\phi^- - \psi\right) \\ -\sin\left(\phi^- - \psi\right) \end{bmatrix} + X^+ \begin{bmatrix} \cos\left(2\omega t + \phi^+ - \psi\right) \\ \sin\left(2\omega t + \phi^+ - \psi\right) \end{bmatrix} \quad (2)$$

where x_d^+, x_q^+, x_d^- and x_q^- are voltages or currents in positive and negative dq-frames, X^+ and X^- denote amplitudes of positive and negative sequences respectively, ϕ^+ and ϕ^- are phase shifts of positive and negative sequence components, ψ is the phase shift of Park transformation.

If the oscillating terms are filtered with a low-pass or band-stop filter, the phase margin of the system is reduced considerably [3], therefore the above equations are not used directly, but rather as a basis for more efficient techniques.

1) Decoupling by Compensation

This method is based on the fact that the amplitude of the oscillations X^- in (1) is equal to X^- in (2). A similar observation is valid for X^+. It is thus possible to eliminate the oscillations by subtracting them [3]. A combination of a low-pass filter (LPF) and double line frequency Park transforms is used to produce an oscillating signal, which is then subtracted, as shown in Fig. 2-a. The blocks C and P represent the Clarke and Park transformations, and the superscripts ±1 and ±2 correspond to direct and inverse transformation at line frequency and double line frequency.

If the reference values for currents in dq-frames are supposed to be constant, they can be taken as feedforward terms, in this case filtering sould only be applied to the error signal between measured and reference currents [3]. Such approach has similar performance.

2) Decoupling in αβ-frame

It is possible to decouple the sequences in the stationary αβ-frame, knowing that in a sinusoidal steady state the following equations are true for positive and negative sequences:

$$x_\alpha^+(t) = -x_\beta^+\left(t - \frac{T}{4}\right), \quad x_\beta^+(t) = x_\alpha^+\left(t - \frac{T}{4}\right) \quad (3)$$

$$x_\alpha^-(t) = x_\beta^-\left(t - \frac{T}{4}\right), \quad x_\beta^-(t) = -x_\alpha^-\left(t - \frac{T}{4}\right) \quad (4)$$

where x_α^+, x_β^+, x_α^- and x_β^- are positive and negative sequences of voltages or currents in αβ-frame, T is the period of fundamental frequency. This gives the following decoupled terms [10]:

$$x_\alpha^+(t) = \frac{1}{2}\left[x_\alpha(t) - x_\beta\left(t - \frac{T}{4}\right)\right], \quad x_\beta^+(t) = \frac{1}{2}\left[x_\beta(t) + x_\alpha\left(t - \frac{T}{4}\right)\right] \quad (5)$$

$$x_\alpha^-(t) = \frac{1}{2}\left[x_\alpha(t) + x_\beta\left(t - \frac{T}{4}\right)\right], \quad x_\beta^-(t) = \frac{1}{2}\left[x_\beta(t) - x_\alpha\left(t - \frac{T}{4}\right)\right] \quad (6)$$

where x_α and x_β are measured voltages or currents in αβ-frame.

Park transformations are then applied to the corresponding extracted sequences to obtain constant signals, as in Fig. 2-b.

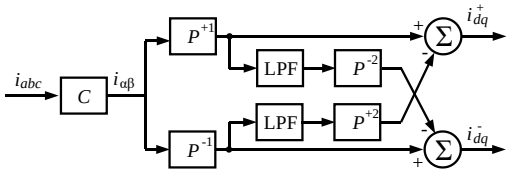

a)

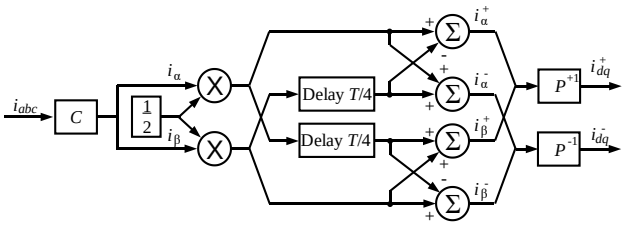

b)

Fig. 2. Sequence decoupling: a) by compensation, b) in αβ-frame

B. Synchronization

The PLL (phase locked loop) is used to synchronize with the AC grid. Based on a feedback loop, it produces the reference angle Θ, that corresponds to the phase of the positive sequence voltage, which is used for Park transformation [3].

Under unbalanced conditions, oscillating values produced by (1) and (2) influence the behavior of the PLL if the instantaneous values are fed directly into the feedback loop. To account for that, several solutions exist, such as preliminary sequence extraction, SOGI-PLL [16] or averaging the feedback variable over one period. The latter is considered in this article.

C. Inner Control

Considering Fig. 1, the following convenience variables are defined for each phase ($j = a, b, c$):

$$v_{conv_{dc}\,j} = v_{u\,j} + v_{l\,j}, \; v_{conv_{ac}\,j} = \frac{v_{l\,j} - v_{u\,j}}{2} \quad (7)$$

$$i_{diff\,j} = \frac{i_{u\,j} + i_{l\,j}}{2} \quad (8)$$

where $i_{u\,j}, i_{l\,j}$ and $v_{u\,j}, v_{l\,j}$ are the currents and the sums of SM voltages in upper and lower arms respectively.

From Fig. 1, (7) and (8), it is possible to deduce [17]:

$$v_j - v_{conv_{ac}\,j} = \left(L_{arm}/2 + L\right)\frac{di_j}{dt} + \left(R_{arm}/2 + R\right)i_j \quad (9)$$

$$V_{dc} - v_{conv dc\,j} = 2L_{arm}\frac{di_{diff\,j}}{dt} + 2R_{arm}i_{diff\,j} \quad (10)$$

where L_{arm} and R_{arm} are arm inductance and resistance; V_{dc} is DC voltage at converter terminals; v_j is the PCC voltage. AC side current control is based on (9), and DC side ripple control is based on (10), as will be explained in the following.

1) Control in dq-frame

To control positive and negative sequence currents, it is possible to use conventional PI regulators in the rotating positive and negative dq-frames with grid voltage and current feedforward to produce reference signals for the grid-side voltage (11), (12). The system for positive dq-frame is shown in Fig. 3 and the negative dq-frame system is analogous.

$$\begin{bmatrix} e_d^+ \\ e_q^+ \end{bmatrix} = \begin{bmatrix} v_d^+ \\ v_q^+ \end{bmatrix} - \begin{bmatrix} PI(s)(i_d^{+ref} - i_d^+) \\ PI(s)(i_q^{+ref} - i_q^+) \end{bmatrix} - \omega\left(\frac{L_{arm}}{2} + L\right)\begin{bmatrix} -i_q^+ \\ i_d^+ \end{bmatrix} \quad (11)$$

$$\begin{bmatrix} e_d^- \\ e_q^- \end{bmatrix} = \begin{bmatrix} v_d^- \\ v_q^- \end{bmatrix} - \begin{bmatrix} PI(s)(i_d^{-ref} - i_d^-) \\ PI(s)(i_q^{-ref} - i_q^-) \end{bmatrix} - \omega\left(\frac{L_{arm}}{2} + L\right)\begin{bmatrix} i_q^- \\ -i_d^- \end{bmatrix} \quad (12)$$

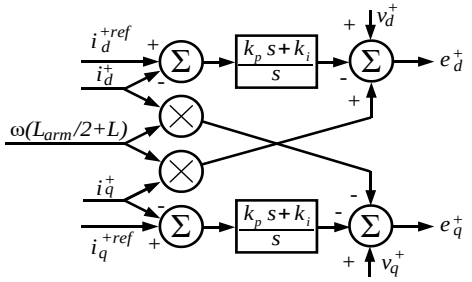

Fig. 3. Control of MMC station currents in positive dq-frame

2) Control in Stationary αβ-frame

Another solution is the implementation of a Proportional-Resonant (PR) controllers (13) in the stationary αβ-frame, as shown in Fig. 4 [14]. If the coefficients k_p and k_i are set to be twice the values of those presented in the section II.C.1, the behavior of the system is equivalent [3].

$$\begin{bmatrix} e_\alpha \\ e_\beta \end{bmatrix} = \begin{bmatrix} v_\alpha \\ v_\beta \end{bmatrix} - \begin{bmatrix} \frac{k_i s}{s^2+\omega^2} + k_p & 0 \\ 0 & \frac{k_i s}{s^2+\omega^2} + k_p \end{bmatrix} \begin{bmatrix} i_\alpha^{ref} - i_\alpha \\ i_\beta^{ref} - i_\beta \end{bmatrix} \quad (13)$$

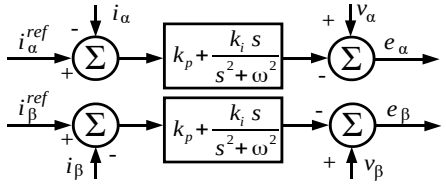

Fig. 4. Control of MMC station currents in stationary αβ-frame

D. Outer Control

In HVDC applications, the outer loop controls active/reactive power and DC voltage, producing the reference currents for the inner loop. Power regulation is based on an integral control with gains k_{iP} and k_{iQ} for active and reactive power (14), (15). If balanced conditions and perfect synchronization is considered, (14) and (15) are used:

$$i_d^{ref} = \frac{1}{v_d}\frac{k_{iP}}{s}\left(P_{ac3}^{ref} - P_{ac3}\right) \quad (14)$$

$$i_q^{ref} = \frac{1}{v_d}\frac{k_{iQ}}{s}\left(Q_{ac3}^{ref} - Q_{ac3}\right) \quad (15)$$

As for the DC voltage, a second order closed loop transfer function is typically used, based on the control equation (16):

$$i_d^{ref} = \left(\frac{k_{i_{Vdc}}}{s} + k_{P_{Vdc}}\right)\left(V_{dc}^{ref} - V_{dc}\right) \quad (16)$$

The DC side current I_{dc} is considered as a constant disturbance that can be rejected with this regulator and therefore is not included in the control equation.

E. Current Reference Distribution

The signals produced by the outer control loop need to be converted to a set of reference currents for the internal loop. Depending on the objective during unbalance, it can be done using different techniques [3], [5], described in the following.

The methods discussed in this paper are based on the following matrix equation for active/reactive powers, voltages and currents at PCC in dq-frame (pu) values [3]:

$$\begin{bmatrix} \bar{P} \\ \bar{Q} \\ P_{C2} \\ P_{S2} \\ Q_{C2} \\ Q_{S2} \end{bmatrix} = \begin{bmatrix} v_d^+ & v_q^+ & v_d^- & v_q^- \\ v_q^+ & -v_d^+ & v_q^- & -v_d^- \\ v_d^- & v_q^- & v_d^+ & v_q^+ \\ v_q^- & -v_d^- & -v_q^+ & v_d^+ \\ v_q^- & -v_d^- & v_q^+ & -v_d^+ \\ -v_d^- & -v_q^- & v_d^+ & v_q^+ \end{bmatrix} \begin{bmatrix} i_d^+ \\ i_q^+ \\ i_d^- \\ i_q^- \end{bmatrix} \quad (17)$$

where $\bar{P}$ and $\bar{Q}$ are the average values over one period, P_{C2}, P_{S2}, Q_{C2} and Q_{S2} are the amplitudes of the second harmonic oscillatory terms in phase and in quadrature with positive sequence voltage.

1) PNSC (Positive Negative Sequence Control)

This approach allows to suppress active/reactive power ripple when the reference of reactive/active power is zero:

$$\begin{bmatrix} i_d^+ \\ i_q^+ \\ i_d^- \\ i_q^- \end{bmatrix} = \frac{1}{\left|v^+\right|^2 - \left|v^-\right|^2} \begin{bmatrix} v_d^+ & v_q^+ \\ v_q^+ & -v_d^+ \\ -v_d^- & v_q^- \\ -v_q^- & -v_d^- \end{bmatrix} \begin{bmatrix} \bar{P} \\ \bar{Q} \end{bmatrix} \quad (18)$$

If the amplitude of positive sequence voltage is equal to the amplitude of the negative sequence voltage, which is the case during close phase-to-phase faults, division by zero occurs, therefore (18) should be used with care in real applications.

2) AARC (Average Active-Reactive Control)

This control method allows the injection of minimal RMS currents needed to produce the necessary average active and reactive power:

$$\begin{bmatrix} i_d^+ \\ i_q^+ \\ i_d^- \\ i_q^- \end{bmatrix} = \frac{1}{\left|v^+\right|^2 + \left|v^-\right|^2} \begin{bmatrix} v_d^+ & v_q^+ \\ v_q^+ & -v_d^+ \\ v_d^- & -v_q^- \\ v_q^- & v_d^- \end{bmatrix} \begin{bmatrix} \bar{P} \\ \bar{Q} \end{bmatrix} \quad (19)$$

3) BPSC (Balanced Positive Sequence Control)

This approach allows the injection of balanced positive sequence currents, producing the necessary average active and reactive powers:

$$\begin{bmatrix} i_d^+ \\ i_q^+ \end{bmatrix} = \frac{1}{\left|v^+\right|^2} \begin{bmatrix} v_d^+ & v_q^+ \\ v_q^+ & -v_d^+ \end{bmatrix} \begin{bmatrix} \bar{P} \\ \bar{Q} \end{bmatrix} \tag{20}$$

$$i_d^- = i_q^- = 0 \tag{21}$$

4) FPNSC (Flexible Positive Negative Sequence Control)

This control method allows to transmit the desired fraction of the total power through each sequence. The coefficients k_P and k_Q define the proportion of active and reactive powers transmitted by the positive sequence. The negative sequence currents have to transmit $(1-k_P)$ and $(1-k_Q)$ of active and reactive powers:

$$\begin{bmatrix} i_d^+ \\ i_q^+ \end{bmatrix} = \frac{1}{\left|v^+\right|^2} \begin{bmatrix} v_d^+ & v_q^+ \\ v_q^+ & -v_d^+ \end{bmatrix} \begin{bmatrix} k_P\bar{P} \\ k_Q\bar{Q} \end{bmatrix} \tag{22}$$

$$\begin{bmatrix} i_d^- \\ i_q^- \end{bmatrix} = \frac{1}{\left|v^-\right|^2} \begin{bmatrix} v_d^- & -v_q^- \\ v_q^- & v_d^- \end{bmatrix} \begin{bmatrix} (1-k_P)\bar{P} \\ (1-k_Q)\bar{Q} \end{bmatrix} \tag{23}$$

Changing the coefficients allows imitating all strategies.

If the grid voltage is balanced, it is not possible to transmit power through the negative sequence currents, as $v_d^- = v_q^- = 0$.

F. Proposed DC Side Ripple Suppression Control

In balanced conditions, the DC current is found from:

$$I_{dc} = \sum_j i_{diff\ j} \tag{24}$$

Considering (24), (10) is rewritten as follows:

$$V_{dc} - v_{convdc3} = \frac{2}{3} L_{arm} \frac{dI_{dc}}{dt} + \frac{2}{3} R_{arm} I_{dc} \tag{25}$$

The equivalent circuit model is illustrated in Fig. 5-a.

Double line frequency zero sequence currents that propagate to the DC link during unbalance can be regarded separately, using the superposition principle and supposing that the DC voltage at the other substation is constant, Fig. 5-b.

Based on this, a double line frequency ripple controller with cascaded structure is proposed: the inner controller ($PR1$) is for DC current and the external controller ($PR2$) is for DC voltage ripple suppression, as shown in Fig. 5-c, where variables having the index 0 denote the zero sequence of double line frequency.

The resulting control function is as follows:

$$e_0 = \left((0 - V_{dc0})PR2(s) - i_0\right)PR1(s) \tag{26}$$

$$PR1(s) = \frac{k_{i1}s}{s^2 + (2\omega)^2} + k_{p1}, \quad PR2(s) = \frac{k_{i2}s}{s^2 + (2\omega)^2} + k_{p2} \tag{27}$$

The value of e_0 is added to the references obtained with AC side current regulators discussed previously (Section II.C) to produce the final arm voltage references of MMC.

III. Simulation Case Study

The control blocks discussed earlier are implemented in the EMTP-RV simulation environment [18] and compared on a simple test case of a point-to-point HVDC link (Fig. 6). The power is transferred from VSC2 (rectifier, P and Q controls) to VSC1 (inverter, V_{dc} and Q controls). A single-line-to-ground (SLG) fault at a transformer terminal causes grid unbalance.

A. Sequence Decoupling

To test the decoupling blocks (Section II.A), an initially balanced three-phase system is applied and then phase A voltage drops to zero at 0.5 s, Fig. 7. The responses are shown in Fig. 8.

Decoupling in αβ-frame gives a constant response time equal to ¼ of a period of fundamental frequency, while that of decoupling by compensation depends on filter tuning and produces overshoots and oscillations.

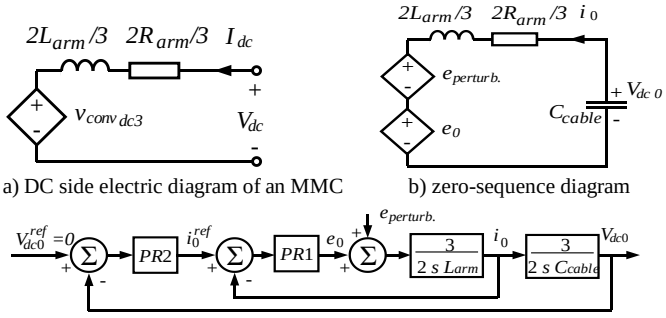

a) DC side electric diagram of an MMC b) zero-sequence diagram

c) proposed controller

Fig. 5. DC side double line frequency suppression

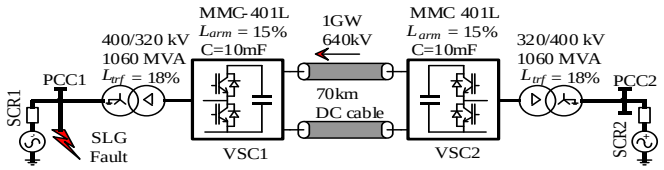

Fig. 6. Simulated point-to-point HVDC link

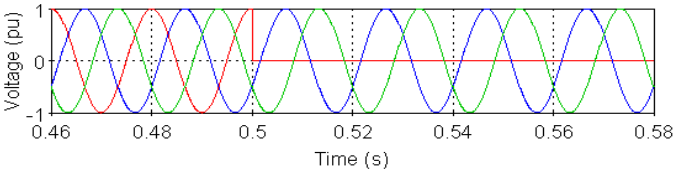

Fig. 7. Voltage during SLG fault on phase A at 0.5 s

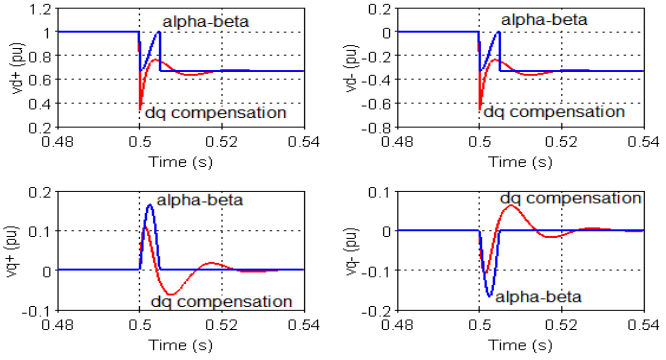

Fig. 8. Voltage sequence decoupling during SLG fault on phase A at 0.5 s

B. Current Control

PR controllers in αβ-frame and PI controllers in decoupled positive and negative dq-frames (Section II.C) are compared in Fig. 9. They are tuned for 10 ms response time and a damping factor of 0.707. The reference values for currents in pu are: $i_d^+ = 0.5$, $i_q^+ = i_d^- = i_q^- = 0$.

PR controllers and decoupled PI controllers are able to maintain the system in the desired state without noticeable oscillations of current, their performances are equivalent.

C. Reference Distribution

This section compares the reference distribution strategies presented in the Section II.E on an SLG fault on phase A at PCC1 at t = 0.5 s, Fig. 6. Reference values for the two stations in pu are as follows: $P_{MMC1}=0.25$, $Q_{MMC1}=0$, $V_{dcMMC2}=1$ and $Q_{MMC2}=0$. Although FRT norms require reactive power injection during faults, such values are set for simplicity.

The results are evaluated comparing AC side currents in decoupled dq-frames, Fig. 10; active and reactive powers, Fig. 11; and AC side currents of the station MMC1, Fig. 12.

With PNSC strategy, the active power is constant, since the reference for the reactive power is zero (necessary condition to suppress active power ripple). AC side currents have the highest amplitudes. AARC strategy produces the smallest RMS values of AC side currents (≈0.35 pu), reactive power ripple is eliminated. With BPSC strategy, the AC side currents are balanced, instantaneous active and reactive powers oscillate at double line frequency with equal amplitude.

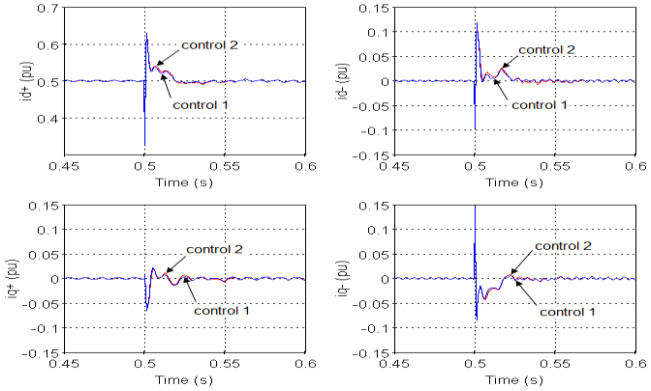

Fig. 9. Current control in case of SLG fault on phase A at 0.5 s: control 1 – PR-controller, control 2 – PI controllers in decoupled dq-frames

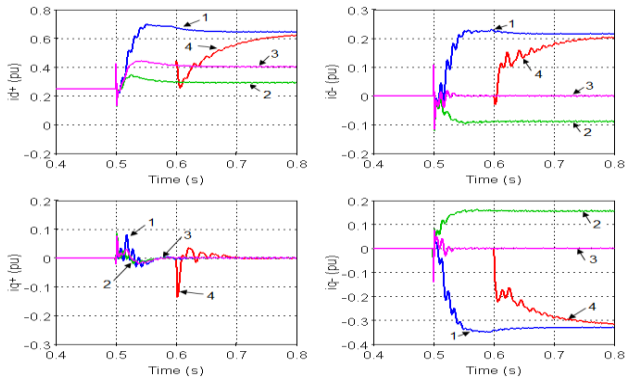

Fig. 10. Comparison of AC side currents in decoupled dq-frames for different strategies: 1 – PNSC, 2 – AARC, 3 – BPSC, 4 – FPNSC

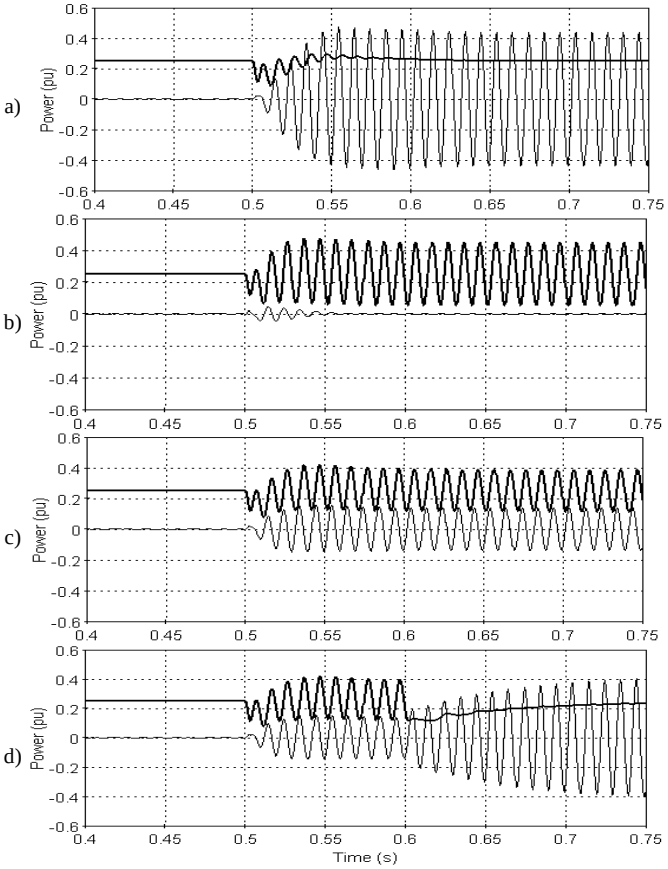

Fig. 11. Active (bold) and reactive power for different reference distribution strategies during unbalance: a) PNSC, b) AARC, c) BPSC, d) FPNSC

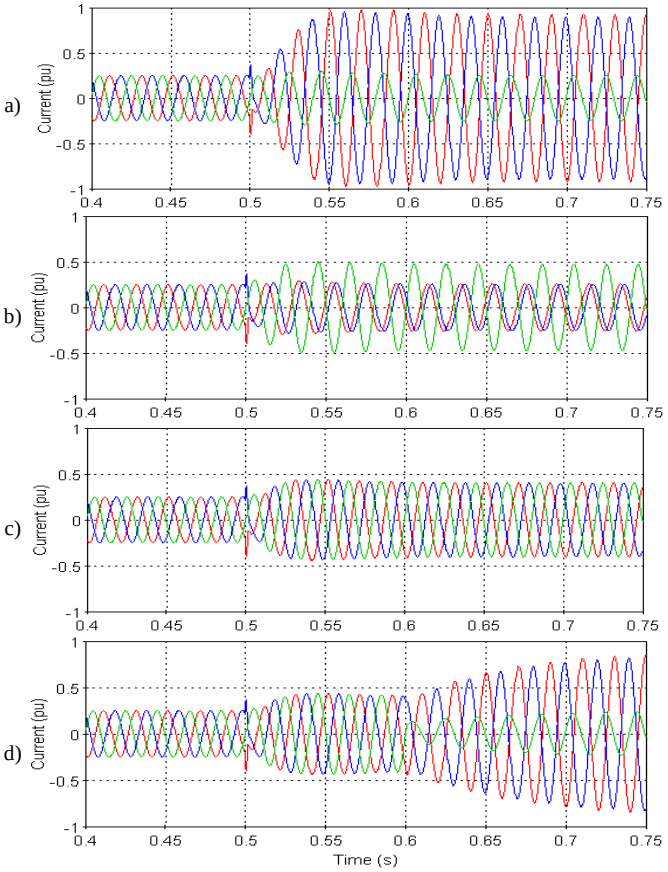

Fig. 12. AC side currents in abc-frame for different reference distribution strategies during unbalance: a) PNSC, b) AARC, c) BPSC, d) FPNSC

The flexibility of FPNSC strategy is demonstrated as follows: the coefficients k_P and k_Q are initially set to 1 (the power is transmitted via the positive sequence), which gives the same result as BPSC, since no negative sequence current is injected. At 0.6 s a change $k_P = 0.73$ is applied, which eliminates active power ripple, imitating PNSC.

D. DC side Ripple Suppression Controller

This section demonstrates the developed DC side double line frequency ripple suppression controller proposed in Section II.F, on an SLG fault on phase A at PCC1.

The results of the simulation are shown in Fig. 13. It can be observed that the oscillations of DC side voltage and current are successfully eliminated with the developed controller. Similar results are obtained for unbalanced faults applied at VSC2 station.

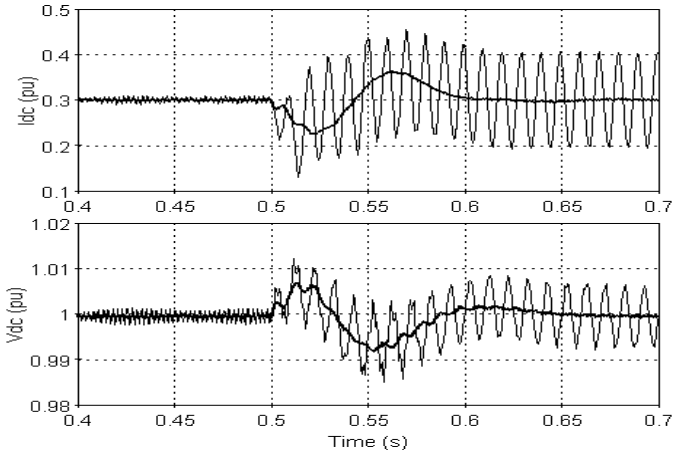

Fig. 13. Evaluation of DC side ripple suppression controller. Bold line – controller applied, narrow line – controller not applied

IV. Conclusion

This article presents a review of some widely applied MMC control techniques under unbalanced grid conditions.

Sequence decoupling can be performed by compensation in dq-frame and produces oscillations and overshoots. The delay-based decoupling in αβ-frame has constant response time.

The classical cascade control structure can be adapted to operate under unbalanced conditions by decoupling positive and negative sequence currents and adding a separate set of PI controllers for the negative sequence, or applying PR controllers in the stationary αβ-frame. With proper choice of coefficients, their performances can be equivalent.

Different control objectives can be applied, such as suppression of active/reactive power oscillations or producing a set of balanced positive sequence AC currents. Active power ripple suppression is not possible when the amplitudes of positive and negative sequence voltages are equal.

Contrary to the conventional 2- and 3-level VSC converters, even when the instantaneous AC power of an MMC converter oscillates (for example, balanced positive sequence currents injection during a phase-to-ground fault), the DC side of the converter is not affected if a proper zero-sequence controller is applied.

The developed DC side double line frequency controller eliminates oscillations during grid unbalance.

V. References

[1] A. Lesnicar and R. Marquardt, "An innovative modular multilevel converter topology suitable for a wide power range," in *Proc. 2003 IEEE Bologna Power Tech Conference*, vol. 3, pp. 1-6.

[2] H. Saad, "Modélisation et simulation temps réel d'une liaison HVDC de type VSC-MMC," Ph.D. dissertation, Polytechnique Montréal, 2015.

[3] R. Teodorescu, M. Liserre and P. Rodriguez, *Grid Converters for Photovoltaic and Wind Power Systems*, John Wiley & Sons, 2011.

[4] M. Guan and Zh. Xu, "Modeling and control of a modular multilevel converter-based HVDC system under unbalanced grid conditions," *IEEE Trans. Power Electron*., vol. 27, issue 12, pp. 4858-4867, Apr. 2012.

[5] K. Ma, W. Chen, M. Liserre and F. Blaabjerg, "Power controllability of a three-phase converter with an unbalanced AC source," *IEEE Trans. Power Electron.*, vol. 30, issue 3, pp. 1591-1604, Mar. 2015.

[6] A. Timofejevs, D. Gamboa, M. Liserre, R. Teodorescu and S. K. Chaudhary, "Control of transformerless MMC-HVDC during asymertic grid faults," in *IEEE 2013 Industrial Electronics Society, IECON - 39th Annual Conf.*, pp. 2016-2021.

[7] R. Teodoresku, F. Blaabjerg and M. Liserre, "Proportional-Resonant Controllers. A new breed of controllers suitable for grid-connected voltage-source converters," in *Proc. 2004 International Conference on Optimization of Electrical and Electronic Equipments, Optim*, pp. 9-14.

[8] Y. Yan, M. Wang, Z.-F. Song and C.-L. Xia, "Proportional-resonant control of doubly-fed induction generator wind turbines for low-voltage ride-through enhancement," *Energies*, vol. 5, pp. 4758-4778, Nov. 2012.

[9] S. Podrucky, "Small signal modeling of resonant controlled VSC systems," M.Sc. dissertation, University of Toronto, 2009.

[10] C. Du, A. Sannino and M. H.J. Bollen, "Analysis of response of VSC-based HVDC to unbalanced faults with different control systems," in *Proc. IEEE/PES 2005 Transmission and Distribution Conference & Exposition: Asia and Pacific*, pp. 1-6.

[11] G. Bergna, J. A. Suul, E. Bernet, P. Egrot, J.-C. Vannier, and M. Molinas, "Analysis of modular multilevel converters under unbalanced grid conditions with different load current control strategies and Lagrange-based differential current control," in *Proc. 2013 1st International Future Energy Electronics Conference*, pp. 669-674.

[12] J. Hu, W. Zhang, H. Wang, Y. He and L. Xu, "Proportional integral plus multi-frequency resonant current controller for grid-connected voltage source converter under imbalanced and distorted supply voltage conditions," *Journal of Zhejiang University SCIENCE A*, vol. 10, issue 10, pp. 1532-1540, Oct. 2009.

[13] Q. Tu, Z. Xu, Y. Chang and L. Guan, "Suppressing DC voltage ripples of MMC-HVDC under unbalanced grid conditions," *IEEE Trans. Power Del.*, vol. 27, issue 3, pp. 1332-1338, June 2012.

[14] Z. Yuebin, J. Daozhuo, G. Jie, H. Pengfei and L. Zhiyong, "Control of modular multilevel converter based on stationary frame under unbalanced AC system," in *Proc. 2012 Third International Conference on Digital Manufacturing and Automation (ICDMA)*, pp. 293-296.

[15] H. Saad, J. Peralta, S. Dennetière, J. Mahseredjian, J. Jatskevich, J. A. Martinez, A. Davoudi, M. Saeedifard, V. Sood, X. Wang, J. Cano and A. Mehrizi-Sani, "Dynamic averaged and simplified models for MMC-based HVDC transmission systems," *IEEE Trans. Power Del.*, vol. 28, issue 3, pp. 1723-1730, Apr. 2013.

[16] M. Ciobotaru, R. Teodorescu and F. Blaabjerg, "A new single-phase PLL structure based on second order generalized integrator," in *Proc. IEEE 2006 Power Electronics Specialists Conference PESC*, pp. 1-6.

[17] H. Saad, X. Guillaud, J. Mahseredjian, S. Dennetiere and S. Nguefeu, "MMC capacitor voltage decoupling and balancing controls," *IEEE Trans. Power Del.*, vol. 30, issue 2, pp. 704-712, July 2014.

[18] J. Mahseredjian, S. Dennetière, L. Dubé, B. Khodabakhchian and L. Gérin-Lajoie, "On a new approach for the simulation of transients in power systems," *Electric Power Systems Research*, vol. 77, issue 11, pp. 1514-1520, Sep. 2007.